

1 **The impact of land cover generated by a dynamic**
2 **vegetation model on climate over East Asia in present and**
3 **possible future climate**

4
5 **Mee-Hyun Cho¹, Kyung-On Boo², G. M. Martin³, Johan Lee², Gyu-Ho Lim¹**

6
7 [1]{School of Earth and Environmental Sciences, Seoul National University, Seoul, Republic
8 of Korea}

9 [2] {National Institute of Meteorological Research, Korea Meteorological Administration,
10 Seoul, Republic of Korea}

11 [3] {Met Office Hadley Centre, FitzRoy Road, Exeter, UK}

12 Correspondence to: M.-H. Cho (mhjo77@snu.ac.kr)

13
14 **Abstract**

15 This study investigates the impacts of land cover change, as simulated by a dynamic vegetation
16 model, on the summertime climatology over Asia. The climate model used in this study has
17 systematic biases of underestimated rainfall around Korea and overestimation over the South
18 China Sea. When coupled to a dynamic vegetation model, the resulting change in land cover is
19 accompanied by an additional direct radiative effect over dust-producing regions. Both the
20 change in land surface conditions directly and the effect of increased bare soil fraction on dust
21 loading, affect the climate in the region, and are examined separately in this study. The direct
22 radiative effect of the additional dust contributes to increasing the rainfall biases, while the land
23 surface physical processes are related to local temperature biases such as warm biases over

24 North China. In time-slice runs for future climate, as the dust loading changes, anomalous
25 anticyclonic flows are simulated over South China Sea, resulting in reduced rainfall over the
26 South China Sea and more rainfall toward around Korea and South China. In contrast with the
27 rainfall changes, the influence of land cover change and the associated dust radiative effects
28 are very small for future projection of temperature, which is dominated by atmospheric CO₂
29 increase. The results in this study suggest that the land cover simulated by a dynamic vegetation
30 model can affect, and be affected by, model systematic biases on regional scales over dust
31 emission source regions such as Asia. In particular, analysis of the radiative effects of dust
32 changes associated with land cover change is important in order to understand future changes
33 of regional precipitation in global warming.

34

35 **1 Introduction**

36 Bordered by the Tibetan Plateau to the west, the Eurasian land mass to the northwest, and the
37 vast Pacific Ocean to the south and east, East Asia has experienced one of the most pronounced
38 monsoon climates of the globe for centuries (Lau and Li, 1984). Land surface properties are
39 important because of their known impact on the East Asian monsoon circulation (Kang and
40 Hong, 2008; Lee et al., 2011) and on the Indian monsoon (Douglas et al., 2006; Lee et al., 2009;
41 Battle Bayer et al., 2012; Martin and Levine, 2012). Lee et al. (2011) proposed that a
42 replacement of vegetation with bare soil would cause an associated decrease in latent heat
43 during the summer, which could weaken East Asian monsoon circulation. This decrease in
44 latent heat flux over land could weaken the East Asian monsoon via a positive feedback
45 between the latent heat flux contrast and rainfall. Yamashima et al. (2011) showed a similar
46 study over the Indian subcontinent and Southeastern China. Land surface property changes
47 from forest to cultivated land have resulted in a decrease in the monsoon rainfall and provoked
48 an associated weakening of the Asian summer monsoon circulation. Moreover, there are a few
49 studies investigating the influence of land cover change that have demonstrated significant
50 impact on East Asian Monsoon (Kang et al., 2005), but they usually used satellite-based (Suh
51 and Lee, 2004; Kang and Hong, 2008) and idealized land cover change (Lee et al., 2011).

52 Although Earth System models with dynamic vegetation schemes allow representation of the
53 carbon cycle feedbacks on climate, the land cover distribution could also be influenced by, and
54 indeed influence, model systematic biases (Martin and Levine, 2012, hereafter ML12). Land
55 surface property changes have effects on the atmosphere through physical processes (such as
56 changes in surface roughness, albedo and evapotranspiration), and can induce additional
57 indirect impacts when coupled with aerosol processes as well. For example, changes in surface
58 emissions of mineral dust that are caused by changes in bare soil fraction will have a radiative
59 effect in the atmosphere. Additional dust loading of the atmosphere resulting from land cover
60 change in an Earth System model could, therefore, add to the model uncertainty via feedbacks
61 with model systematic biases such as lack of rainfall over dust-producing regions. Dust affects
62 both shortwave and longwave radiative fluxes, and the effects of mineral dust on the radiation
63 budget are important due to the widespread distribution and large optical depth of mineral dust
64 (Sokolik and Toon, 1996). A study by Yoshioka et al. (2007) suggests that the direct radiative
65 forcing of dust can explain up to 30% of the observed precipitation reduction in the Sahel in
66 three decadal scale simulation. Dust is removed from the atmosphere by both dry and wet
67 deposition processes, providing a source of iron to phytoplankton and thus potentially affecting
68 the carbon cycle (Collins et al., 2011). Since Northeast Asia is one of the major dust emission
69 source regions, land surface property changes over this source region need to be studied.
70 Aerosol, as one of the fundamental atmospheric constituents, has an important impact on the
71 climate system. Ramanathan et al. (2005) showed that global dimming causes a long-term
72 (multi-decadal) weakening of the South Asian monsoon by reducing the meridional surface
73 temperature gradient between the Asian land mass and the Indian Ocean. Aerosol affects
74 precipitation events through cloud physics processes in China (Qian et al., 2009), while dust
75 can also contribute to Asian monsoon rainfall anomalies by heating the upper troposphere (Lau
76 et al., 2006, Lau and Kim, 2006). Therefore, aerosol impacts due to land cover changes may
77 be important in regional climate over East Asia.

78 ML12 investigated the impacts on climate of land cover changes, and associated dust effects,
79 that resulted from model systematic biases. Their results reflect that over dust producing
80 regions, land cover change simulated by a Dynamic Global Vegetation Model (DGVM) can
81 affect both the present-day simulation and the future response as well. According to Hurrell et

82 al. (2009) and McCarthy et al. (2012), since model systematic biases affect climate model
83 sensitivity, we need to study processes related to systematic biases in order to understand future
84 climate projections. Motivated by ML12, this study extends ML12 by applying their results for
85 East Asia. The aims of this study are: first, to investigate the physical influence of changes in
86 land cover conditions and associated changes in aerosol loading on the rainfall and surface
87 temperature over East Asia; and second, to provide insight into the possible conflicting
88 contributions to uncertainty in climate projections for the region that come from the inclusion
89 of dynamic vegetation in a climate model (which ought to be beneficial) and its interaction
90 with existing precipitation biases (which is detrimental).

91 The present paper is organized as follows. Section 2 briefly describes the global circulation
92 model used in this study, the experimental design, and the data. The results of the study are
93 given in section 3. The impact of land cover distribution and radiative effect of dust under
94 present and possible future climate are all provided in this section. A summary and discussion
95 are given in section 4.

96

97 **2 Model Experimental Design and Data**

98 In this study, we used the same datasets as used in ML12, and we follow a similar methodology
99 for the analysis, with additional investigation of particular aspects concerning the East Asian
100 region. The experiments were produced using the Hadley Centre Global Environmental Model
101 version 2 (HadGEM2) model family that had been developed by the UK Met Office (The
102 HadGEM2 Development Team, 2011). The horizontal grid interval was $1.25^{\circ} \times 1.875^{\circ}$ in the
103 latitude-longitude directions, and 38 vertical layers were used with the top of atmosphere over
104 39 km in height. The land surface scheme in the HadGEM2 family is a tiled version of the Met
105 Office Surface Exchange Scheme (MOSES) version 2, which represents heterogeneous surface
106 properties (Cox et al., 1999; Essery and Clark, 2003). A grid box represents a mixture of five
107 vegetation or plant-functional types (PFTs), which include broadleaf trees, needleleaf trees,
108 temperate C₃ grass, tropical C₄ grass, and shrubs, and four non-vegetated surface types, which
109 include urban, inland water, bare soil, and ice. Surface fluxes and temperatures are calculated

110 separately for each surface type and are aggregated according to each tile's fractional coverage
111 before being passed to the atmospheric model (Lawrence and Slingo, 2004).

112 The experiment configuration used by ML12 is as follows. For the present-day (1980-2005)
113 runs, the HadGEM2 atmosphere-only model was forced with observed sea surface
114 temperatures (SSTs) and sea ice. The experimental design and forcing datasets are as specified
115 by the Fifth Coupled Model Intercomparison Project (CMIP5) and are detailed in Taylor et al.
116 (2012). The land cover and vegetation types were prescribed by the International Geophysical
117 Biophysical Programme (IGBP; Loveland et al., 2000) with a prescribed seasonally-varying
118 leaf area index (LAI) based on Moderate Resolution Imaging Spectroradiometer (MODIS)
119 Terra Collection 5 monthly LAI datasets. Historical land use change information based on
120 CMIP5, provided to CMIP5 by the Land Use Harmonization team (Hurtt et al., 2011), were
121 applied by Baek et al. (2013) to the IGBP land cover data in order to prescribe time-varying
122 land cover fields for HadGEM2-A. This is referred to as the "A" experiment.

123 For the future timeslice experiments, the atmosphere component is forced with CO₂ and trace
124 gases for the year 2100 based on the Representative Concentration Pathway (RCP) 8.5 scenario
125 of the CMIP5 (Taylor et al., 2012). The SSTs were obtained by applying the difference between
126 30-year mean SSTs centred around 2100 (from the HadGEM2 Earth System (HadGEM2-ES)
127 RCP8.5 scenario coupled model run) and 30-years mean SSTs centred around 1990 (from the
128 HadGEM2-ES historical run), to the present-day monthly-varying observed SSTs from 1980–
129 2005. The projected future land use changes for the period 2080-2110 based on CMIP5 RCP8.5
130 scenarios were applied in order to prescribe time-varying land cover fields (Hurtt et al., 2011)
131 for HadGEM2-A timeslice experiment. This is referred to as the "Ats" experiment.

132 In addition to the "A" and "Ats" experiments, alternative representations of global vegetation
133 cover from a DGVM were used as the land cover component for further HadGEM2-A
134 experiments under present-day and future climates. In these experiments, the only change made
135 is that the monthly mean land cover information from the HadGEM2-ES historical and RCP8.5
136 runs is used in HadGEM2-A in place of the standard land cover distribution as described above.
137 The HadGEM2-ES configuration uses the Top-down Representation of Interactive Foliage and
138 Flora Including Dynamics (TRIFFID) dynamic vegetation model (Cox, 2001) to simulate the

139 land cover changes from the pre-industrial control period through the present-day and into the
140 future following the CMIP5 RCP scenarios, and land use changes from Hurtt et al. (2011) are
141 applied as disturbances (see Jones et al., 2011 for more details). Therefore, in these additional
142 experiments, the variations in land cover with time during these periods in HadGEM2-ES are
143 experienced by HadGEM2-A, but there is no interactive terrestrial carbon cycle and no
144 feedbacks on the land cover. Variations in land cover from years 1980–2005 of HadGEM2-ES
145 are used in the present-day experiment of this type, referred to as “AE”, while the variations in
146 land cover from years 2080-2110 of HadGEM2-ES are applied to the future timeslice
147 experiment denoted “AEts”. Note that crops are not represented explicitly in HadGEM2-ES;
148 crop and pasture are assumed to be a combination of C₃ and C₄ grass. Details of how land use
149 changes relating to cropland are applied in HadGEM2-ES are given in Jones et al. (2011). This
150 simplification could affect the sensitivity to land cover changes in East Asia in our experiments.

151 A mineral dust scheme (Woodward, 2011) is included in the HadGEM2 model family
152 (HadGEM2 Development Team, 2011) which permits the simulation of changes in mineral
153 dust concentration in response to changes in surface conditions as well as its interaction with
154 model climate via radiative effects. According to ML12, the AE experiment shows a large
155 increase in dust, which is generated as a result of the feedback between the interactive
156 vegetation and the model's systematic rainfall biases in dust-producing regions. Dust is only
157 emitted from the bare soil fraction of a grid-box, and therefore is sensitive to changes to this
158 fraction when the DGVM is used. To evaluate the radiative effects of the dust, an additional
159 pair of experiments was carried out where the direct radiative effects of the dust were switched
160 off. This reduces the dust to a passive tracer in the model with no feedback on the climate.
161 These experiments have the suffix “nod” meaning “no dust radiative effects”. Therefore,
162 “Anod” means a HadGEM2-A simulation with the standard land cover distribution in the
163 present-day, “AEnod” means a HadGEM2-A present-day simulation with HadGEM2-ES land
164 cover without the direct radiative effects of the dust, and “AEnodts” means a HadGEM2-A
165 future timeslice simulation with HadGEM2-ES land cover without the direct radiative effects
166 of dust. The total experiments are listed in Table 1.

167 To compare model results in the present-day runs with observations we used the Global
168 Precipitation Climatology Project (GPCP) precipitation (Alder et al., 2003; Huffman et al.,

169 2009), the CPC Merged Analysis of Precipitation (CMAP, Xie and Arkin, 1997) and the
170 Climatic Research Unit (CRU) mean surface air temperature (Harris et al., 2013). In this study,
171 summer represents the period from June to August.

172

173 **3 Modeling Results**

174

175 **3.1 Present Day**

176 **3.1.1 Impact of ES land Cover on Average Temperature and Precipitations**

177

178 First we examine summer precipitation over East Asia. Figure 1a shows the climatological
179 summertime precipitation distribution of the East Asian summer monsoon. The summer
180 monsoon rainy season evolves with the rainband development covering South China, Korea,
181 Japan and the adjacent seas. Formation of frontal systems is associated with the North Pacific
182 Subtropical High and southwesterlies over the South China Sea. The rainband region, in
183 contrast with the equatorial region, has a small observational uncertainty (Fig. 1b). In Fig. 2,
184 we analyze the North China (NC) region (35-50° N, 105-120° E), Korea (KR) 25-40° N, 120-
185 135° E, and South China (SC) region (20-35° N, 105-120° E), which together represent a large
186 contrast in land cover distribution over East Asia. Simulated precipitation compared with
187 observation (GPCP precipitation) shows a systematic bias in Fig. 2. Precipitation is
188 underestimated over the KR area and overestimated over SC. These spatial features remain in
189 AE, although the underestimated rainfall over KR become larger in AE than A.

190 Figure 3 represents summer surface air temperature bias in the model results compared with
191 the CRU observation data. There is a warm bias greater than 1K in NC and KR, but only a
192 small bias in SC (Fig. 3a). The warm bias over KR is slightly smaller in AE compared to A
193 (Fig. 3c, d). In order to shed light on the bias changes on the regional scale, the land cover
194 difference between AE and A is examined (Fig. 4). Among the five vegetation and bare soil

195 surface types over East Asia, the largest changes are in broadleaf, C₃ grass and bare soil types.
196 Over North China, the increase in bare soil fraction is large. This unrealistic high bare soil
197 fraction has an impact on high dust emission over this region because dust is only emitted from
198 the bare soil fraction of a grid box in this model. In contrast, the South China region is covered
199 by larger broadleaf fraction (Fig. 4) in the AE compared with A, replacing bare soil, shrub and
200 needle-leaf tree. To the north of 50°N, the increase in shrub fraction is distinct (also seen in Fig.
201 4 of ML12).

202 ML12 showed that bare soil area expansion from the changes in the vegetation distribution
203 between AE and A generates additional dust, resulting in a substantial direct radiative impact
204 on the Indian monsoon rainfall. They suggest separate analysis for the dust radiative feedback
205 resulting from land cover change from the analysis of the effects of the change in surface
206 conditions. Accordingly, we examine experiments Anod and AEnod (see Table 1).

207 In Fig. 2, a marked precipitation underestimation over KR is shown compared with
208 observations, particularly when the ES land cover is used. The dry bias amplitudes in summer
209 become larger in AE compared with A (Fig. 2). To estimate the radiative effect of dust on
210 rainfall when the HadGEM2-ES land cover distribution was used, AE was compared with
211 AEnod. The dry bias amplitude of AE decreases in AEnod (Fig. 2c and f) but is still slightly
212 larger than in A. Thus the radiative effect of dust reinforces the dry bias in the KR region
213 (compare Fig. 2b and 2e with Fig. 2c and 2f). This is consistent with the results of ML12 for
214 the South Asian region. ML12 showed significant effects of the change in dust loading on the
215 clear-sky radiative fluxes across South and East Asia (their Fig. 7) and commented on the
216 impacts on surface temperatures which tend to reduce precipitation through cooling of the
217 daytime maxima.

218 To examine the dust radiative effect and land cover change effect in detail, the dry bias in
219 summer over KR in Fig. 2 is considered using Fig. 5. The pattern of changes between "AE-A"
220 in Fig. 5a is similar to the "AE – AEnod" changes (Fig. 5c) rather than those of "AEnod –
221 Anod" (Fig. 5b). This suggests that precipitation over East Asia is more sensitive to the
222 radiative effects of dust associated with land cover changes than to the land cover change alone.

223 In Fig. 6 we make a similar comparison for surface air temperature changes. We find that the
224 dust radiative effect on surface air temperature is associated with a small widespread cooling
225 (Fig. 6c), whereas the surface process effects of the land cover change are associated with a
226 more substantial warming/cooling pattern across the region, as shown in the AEnod-Anod (Fig.
227 6b) and AE-A (Fig. 6a) differences. Over northeastern Eurasia, the increase of shrub fraction
228 replacing broadleaf and needleleaf trees shows a distinct cooling of surface air temperature
229 induced from an increase of surface albedo.

230

231 **3.1.2 Impact of Changes in Land Cover with No Dust Radiative Feedback**

232 To understand more clearly the impacts of the changes in the vegetation distribution in Fig. 6a
233 and 6b, we examined the climate response without the direct radiative effect of dust. The
234 aforementioned increase in warm bias over NC “AEnod–Anod” (Fig. 6b) is considered. Over
235 NC, as the bare soil fraction is larger in AE than A (Fig. 4f; Fig. 7ab), the roughness length
236 reduces while soil evaporation and canopy evaporation decrease. Reduced roughness length
237 induces a decrease of sensible and latent heat fluxes from the surface to the atmosphere (Fig.
238 7c, d, f). The decrease in latent heat flux is associated with reduced cloud amount (Fig. 7e), as
239 well as being favorable for surface warming. As a result, surface air temperature rises over NC
240 (Fig. 7h). The reduced latent heat flux is particularly evident in the canopy evaporation in the
241 NC region, although there is also reduced soil evaporation during the summer (not shown).

242 Similarly, surface cooling over SC and KR is considered in summer. Broadleaf tree fraction
243 expansion (Fig.7b) increases the roughness length (Fig. 7f) and latent heat flux (Fig. 7c),
244 driving surface cooling. While the NC region, where bare soil fraction is increased, showed a
245 decrease of evaporation from A to AE, in the KR and SC regions where broadleaf tree fraction
246 is increased there is increased soil and canopy evaporation from A to AE. These results are
247 consistent with the suggestion by Lee et al (2011) that a vegetation replacement with bare soil
248 would cause an associated decrease in latent heat during the summer. In summary, for the
249 present climate, the land cover effect (bare soil fraction changes in Fig. 7a) is related to surface
250 air temperature changes in summer (Fig. 7h). As bare soil fraction expands (shrinks) the
251 temperature rises (drops).

252 As regards precipitation, Fig. 6 shows only very small changes in precipitation over land in
253 AEnod-Anod (Fig. 6b), and Fig. 10a also shows only small changes in the circulation between
254 these experiments. Thus, the model's direct sensitivity of precipitation to changes in land
255 surface conditions seems to be low compared with the sensitivity to the dust changes that result
256 from them. Although this conclusion is similar to that for India in ML12, the remote influence
257 of changes in springtime Eurasian snow cover associated with the change in vegetation was
258 highlighted for South Asia in that study, whereas for the East Asian region we have shown a
259 more local influence of changes in surface conditions.

260

261 **3.1.3 Impact of Dust Radiative Feedback**

262 We now consider the direct radiative effect of dust resulting from the changes in the vegetation
263 distribution (AEnod-Anod and AE-AEnod of Fig. 8). Concerning the regional climate response,
264 the dust direct radiative effects (Fig. 8b) lead to anomalous northeasterly coastal flow
265 counteracting the summertime climatological monsoonal circulation associated with the
266 western North Pacific high, known to be important in the East Asian summer monsoon rainfall
267 (Lee et al. (2006) and Fig. 8c). The sea level pressure and wind anomalies in "AE - AEnod"
268 are stronger than those of "AEnod - Anod" (Fig. 8a and b), illustrating that the radiative effects
269 of the dust have a larger impact than the surface vegetation changes themselves.

270 The direct radiative effect of dust induces anomalous cyclonic flow over the western North
271 Pacific (KR region in Fig. 8b) that would tend to decrease rainfall over East Asian continent.
272 This is because dust reflects a considerable amount of shortwave radiation, as shown by the
273 increase of upward shortwave radiation at the top of atmosphere (TOA; Fig. 8f), with a
274 resulting cooling the land surface (Fig. 8d). The land surface cooling appears on the continental
275 scale. This is somewhat different from the results in Miller and Tegen (1998) in which they
276 mentioned that the reflected solar flux is offset by the absorption of upwelling longwave
277 radiation, so that the net radiation entering the TOA is only weakly perturbed by dust in
278 comparison to the surface reduction. Although the upward longwave flux is reduced through
279 the dust radiative effects (Fig. 8e), the reduction is smaller than the increase in reflected
280 shortwave at the TOA. Differential heating between land and ocean is one of the fundamental

281 driving mechanisms of the monsoon (Webster et al., 1998). The land-sea thermal contrast
282 becomes weaker due to the direct radiative effect of dust and the pressure contrast weakens.
283 Strong anomalous northeasterly flow along the coast (Fig. 8b), weakening the summer
284 monsoon inflow, induces the dry bias over SC and KR (Fig. 5c). These results seem in line
285 with the argument that dust-induced surface cooling is the dominant mechanism leading to a
286 reduction of precipitation (Konaré et al., 2008; Yoshioka et al., 2007; Paeth and Feichter, 2005).

287

288 **3.2 Future experiments**

289 The effect of including a DGVM, particularly with the feedback on the dust loading, is expected
290 to affect the simulation of future climate change. Changes in AETs relative to AE show
291 increases in rainfall over SC, KR and the western North Pacific (Fig. 9b). Compared with
292 differences between A_{ts} and A in Fig. 9a, Fig. 9b shows a further reduction in rainfall over the
293 South China Sea (SCS) to the south of 20°N accompanied by anticyclonic flow at 850hPa. The
294 discrepancy in future changes in precipitation tends to be larger than that of temperature: Fig.
295 9c and 9d present similar warming patterns.

296 In order to examine the role of different vegetation distributions in global warming, with and
297 without the dust feedbacks, we analyze future timeslice experiments in a similar manner to
298 ML12. To estimate individually the impact of land cover, feedback on the dust loading, and
299 climate change of global warming, we use the experiments described in Table 2. Note that
300 “Dust” and “LCC” are ‘double differences’ illustrating the impacts of the inclusion of the land
301 cover changes, and the radiative effects of the dust changes that the land cover change induces,
302 on the future-present differences.

303 According to Baek et al (2013), the warming and rainfall increment from RCP8.5 are expected
304 to be of the order of $6 \pm 1\text{K}$ and 17% over East Asia. The temperature rises in the timeslice
305 experiments are of similar magnitude (Fig. 9c, 9d, 10b). Consistent with this, Fig. 9 and Fig.
306 10 project a warmer and wetter climate in future summer over NC, KR and SC. Fig. 9b and
307 Fig. 10a show that a larger increase in rainfall between future and present timeslice run is
308 simulated in these regions when land cover change and feedback on the dust are included.

309 However, while precipitation changes over the SCS region tend to be slightly positive on
310 average in climate change-only, including land cover changes and feedback with dust induces
311 a reduction in rainfall in this region.

312 The land surface cover differences in this region between future and present-day climate
313 projected by this model are in C₃ grass expansion replacing bare soil (Fig. 11c, 11f). These
314 changes contribute increases in the evaporation and latent heat flux and decreases in surface
315 air temperature (Fig. 12a, 12b) to the overall future-present changes. Comparison between
316 (AEnodts - AEnod) and (A_{ts}-A) in Fig. 9 showed that the changes in land cover contribute to
317 increased rainfall over the land and reduced rainfall over the SCS. Increasing latent heat flux
318 accompanies lower boundary layer height and is associated with boundary layer moistening
319 (Fig. 12c). According to Lee et al. (2009, 2011), a more vegetated surface tends to be associated
320 with surface moistening, favoring an increase in latent heat and atmospheric moisture (Fig. 12).
321 The changes in vegetation and associated changes in surface air temperature, latent heat fluxes
322 (Fig. 12a and b) and low level circulation (Fig. 12d) are in a similar pattern, but opposite sign,
323 to those shown in Fig. 7c, 7h and 8a. This suggests that the future differences between
324 experiments with different land cover (AEnodts - A_{ts}) are small compared with the present-
325 day differences (AEnod-A) such that the double-difference (AEnodts - AEnod) - (A_{ts} - A)
326 is dominated by the present-day differences. This is consistent with the findings of ML12.

327 In Fig. 12d, increased rainfall over the SC region from 25°N to 35°N is associated with
328 additional anomalous convergence and upward motion over the SC region (see Fig. 13a)
329 induced by the land cover change effect as the monsoon differential circulation results in
330 enhanced moisture transport and cloud formation over SC and KR. In contrast, over the SCS,
331 anomalous anticyclonic flow is related to downward motion from 10°N to 20°N (Fig. 13a) and
332 reduced rainfall (Fig. 12d). The local influence on rainfall of the changes in surface temperature,
333 fluxes and low-level circulation related to the changes in land cover over East Asia are in
334 contrast to the larger-scale responses described in ML12 for South Asia, where the role of
335 future changes in tree cover over northeast Eurasia in the dynamical response associated with
336 the change in meridional temperature gradient was highlighted.

337 As shown in Fig. 10a, the dust radiative forcing is the main contributor to the reduction of
338 simulated precipitation over SCS to the south of 20°N in the AETs future experiment. Figure
339 14 shows the double-difference (AETs minus AE) minus (AEnodts minus AEnod). The
340 atmospheric response shown in Fig. 14 seems to be largely opposite to that in Fig. 8b, 8e and
341 8f, suggesting that it is dominated by the present-day impacts of dust seen between AE and
342 AEnod. In global warming (i.e. future-present), the bare soil fraction decreases (Fig. 11f) so
343 the dust emission of HadGEM2-ES decreases in the future relative to the present climate
344 (Fig.15). As mentioned in Section 3.1.3, the direct radiative effect of dust seems to induce
345 stronger flow than that of ES land cover-only effect. The convective region over SC in the
346 future experiment Aets (Fig. 9a, 13c) is strengthened in AETs (Fig. 9b), and that over the SCS
347 weakened, through the radiative effects of the reduced dust loading (Fig. 13b), with related
348 increases and decreases in precipitation (Fig. 14d and 10a).

349 Overall, for future precipitation projection over East Asia using this model, simulating
350 interactive land cover change by a DGVM, and particularly the subsequent changes in dust
351 radiative effect, are at least as important as the warming conditions. In contrast, for future
352 changes in temperature, the global warming effect is dominant among climate change, land
353 cover change and dust radiative effects over East Asia (Fig. 9c, 9d and 10b).

354

355 **4 Summary and Discussion**

356 In this study, the impact of varying land cover distribution, as simulated by a DGVM, on
357 simulated regional climate over East Asia is examined. The interaction between land cover
358 change by the DGVM and model systematic biases are shown in the present-day climate. The
359 climatology of HadGEM2-A has an underestimation of rainfall over KR in summer and an
360 overestimation over SC. When the land cover from HadGEM2-ES, which uses an interactive
361 vegetation model, is used as an input to HadGEM2-A (experiment AE), the precipitation bias
362 is enhanced over KR and SCS. The difference between AE and A is related to regional bare
363 soil expansion by the DGVM through interaction with the rainfall bias, and also through
364 feedback with the subsequent dust loading, causing a direct radiative effect. The direct radiative

365 effect of dust has an important influence on both the precipitation bias and the stronger
366 circulation response in SLP and wind than the land cover-only effect does. In this study, more
367 dust loading due to excessive bare soil fraction induces an amplified dry bias over Asia. The
368 land cover difference between AE and A affects the surface air temperature bias. In summer, a
369 warm bias in NC (Fig. 7h) is due to bare soil area expansion replacing vegetation (Fig. 7). Soil
370 fraction expands (shrinks) and temperature rises (drops) over NC (SC) (Fig. 7) through changes
371 in surface roughness, evaporation and latent heat fluxes.

372 The dust loading is expected to reduce in the future time-slice run, since C₃ grass replaces bare
373 soil area over NC. The consequent direct radiative effect of dust changes induces the opposite
374 direction of anomalous wind flow over the SCS compared with that induced by the CO₂
375 increase alone. Thus, in the future projection, suppressed rainfall appears over the SCS. Just as
376 the direct radiative effect is significant in the future precipitation simulation, the land cover
377 effect is also important. The C₃ grass expansion replacing bare soil, inducing an increase in
378 latent heat flux, lowers the surface temperature. The changes in land cover between future and
379 present day tend to oppose the surface warming over NC and KR in summer that are driven by
380 increasing CO₂ in the time-slice experiments. When the land cover change impacts and
381 associated dust radiative effect are combined, the resulting rainfall under future climate differs
382 regionally. In contrast with the precipitation response, the temperature response in the time-
383 slice run is dominated by the warming induced from the atmospheric CO₂ increase. In terms of
384 the projected temperature rise, the ES land cover and dust radiative effects are very small.
385 Overall, the inclusion of land cover changes as simulated by an interactive vegetation model
386 has impacts on both present and future climate in East Asia. These results are similar to those
387 for India shown in ML12, although the response amplitude is different. In addition, local rather
388 than remote mechanisms appear to influence the precipitation and circulation response in this
389 region, whereas for India the role of land cover changes in northern Eurasia on the large-scale
390 meridional temperature gradient was highlighted in ML12.

391 Inclusion of dynamic vegetation components in a climate model allows impacts of climate
392 change on both atmospheric composition and ecosystems. When the various feedbacks among
393 the model components are included, complexity increases and the feedbacks affect more
394 numerous systematic biases in models and future climate projections (ML12). As discussed in

395 ML12, as additional Earth System processes are included in a model, the complex interactions
396 and feedbacks between these additional parameterized processes and the model's existing
397 systematic biases, in e.g. rainfall, can be an additional source of uncertainty in climate
398 projection. Therefore it is imperative that model developers continue to strive to improve
399 physical parameterizations in modelling systems. We would emphasize that the details of our
400 results may be dependent on the particular modelling system used for this study. Experiments
401 with more subtle or realistic possible land cover changes have not been carried out for this
402 region with this model, and studies of the influence of vegetation changes using other models
403 (e.g. Lee et al., 2011) have not examined the feedbacks on dust. Therefore, we are unable to
404 speculate on the relative importance of the dust feedback effects under more subtle or realistic
405 possible land cover change scenarios. Nevertheless our results suggest that vegetation
406 feedbacks may be important over East Asia, particularly in the dust emission source regions,
407 for present-day and future climate simulation. Thus, we encourage other modelling centres to
408 investigate these responses in other models where the biases may be different.

409

410 **Acknowledgments**

411 This research was supported by the National Institute of Meteorological Research, Korea
412 Meteorological Administration (project NIMR-2012-B-2), and it used the Unified Model (UM)
413 licence. G.M. Martin was supported by the Joint UK DECC/Defra Met Office Hadley Centre
414 Climate Programme (GA01101) and by the NERC Changing Water Cycle (South Asia) project
415 SAPRISE, grant number NE/I022469/1.

416

417

418 **References**

- 419 Adler, R.F., G.J. Huffman, A. Chang, R. Ferraro, P. Xie, J. Janowiak, B. Rudolf, U. Schneider,
420 S. Curtis, D. Bolvin, A. Gruber, J. Susskind, P. Arkin, E. Nelkin: The Version 2 Global
421 Precipitation Climatology Project (GPCP) Monthly Precipitation Analysis (1979-Present). *J.*
422 *Hydrometeor.*, 4, 1147-1167, 2003.
- 423 Baek, H.-J., J. Lee, H.-S. Lee, C. Cho, W.-T. Kwon, C. Marzin, Y.-K. Hyun, S.-Y. Gan, M.-J.
424 Kim, D.-H. Choi, J. Lee, J. Lee, K.-O. Boo, H.-S. Kang, and Y.-H. Byun: Climate change in
425 the 21st century simulated by HadGEM2-AO under Representative Concentration Pathways,
426 *Asia-Pac. J. Atmos. Sci.*, 49(5), 603-618, 2013.
- 427 Bayer, L. B., B. J. J. M. van den Hurk, B. J. Strengers, and J. G. van Minnen: Regional
428 feedbacks under changing climate and land-use conditions, *Earth Syst. Dynam. Discussions*, 3,
429 201–234, doi:10.5194/esdd-3-201-2012, 2012.
- 430 Cox, P. M., R. A. Betts, C. B. Bunton, R. L. H. Essery, P. R. Rowntree, and J. Smith: The
431 impact of new land surface physics on the GCM simulation of climate and climate sensitivity,
432 *Clim. Dynam.*, 15, 3, 183–203, doi:10.1007/s003820050276, 1999.
- 433 Cox, P. M.: Description of the “TRIFFID” Dynamic Global Vegetation Model, Hadley Centre
434 Technical Note No. 24, available from: [http://www.metoffice.gov.](http://www.metoffice.gov.uk/learning/library/publications/science/climate-science/hadley-centre-technical-note)
435 [uk/learning/library/publications/science/climate-science/hadley-centre-technical-note](http://www.metoffice.gov.uk/learning/library/publications/science/climate-science/hadley-centre-technical-note), last
436 access: 20 July 2012, Met Office Hadley Centre, Exeter, UK, 2001.
- 437 Collins, W. J., Bellouin, N., Doutriaux-Boucher, M., Gedney, N., Halloran, P., Hinton, T.,
438 Hughes, J., Jones, C. D., Joshi, M., Liddicoat, S., Martin, G., O’Connor, F., Rae, J., Senior, C.,
439 Sitch, S., Totterdell, I., Wiltshire, A., and Woodward, S.: Development and evaluation of an
440 Earth-System model – HadGEM2, *Geosci. Model Dev.*, 4, 1051–1075, doi:10.5194/gmd-4-
441 1051-2011, 2011.
- 442 Douglas, E. M., D. Niyogi, S. Frohking, J. B. Yeluripati, R. A. Pielke Sr., N. Niyogi, C. J.
443 Vorosmarty, and U. C. Mohanty: Changes in moisture and energy fluxes due to agricultural

444 land use and irrigation in the Indian Monsoon Belt, *Geophys. Res. Lett.*, 33, L14403,
445 doi:10.1029/2006GL026550, 2006.

446 Essery, R. and D. B. Clark: Developments in the MOSES 2 land-surface model for PILPS 2e,
447 *Global Planet. Change*, 38, 161–164, doi:10.1016/j.bbr.2011.03.031, 2003.

448 Harris, I., Jones, P.D., Osborn, T.J., and Lister, D.H.: Updated high-resolution grids of monthly
449 climatic observations – the CRU TS3.10 Dataset, *Int. J. Climatol.*, 34, 623-642, Doi:
450 10.1002/joc.3711, 2013.

451 Huffman, G.J, R.F. Adler, D.T. Bolvin, G. Gu: Improving the Global Precipitation Record:
452 GPCP Version 2.1, *Geophys. Res. Lett.*, 36, L17808, doi:10.1029/2009GL040000, 2009.

453 Hurrell, J., Meehl, G. A., Bader, D., Delworth, T. L., Kirtman, B., and Wielicki, B.: A unified
454 modeling approach to climate system prediction, *B. Am. Meteorol. Soc.*, 90, 1819–1832,
455 doi:10.1175/2009BAMS2752.1, 2009.

456 Hurtt, G. C., Chini, L. P., Frohking, S., Betts, R., Feddema, J., Fischer, G., Fisk, J. P., Hibbard,
457 K., Houghton, R. A., Janetos, A., Jones, C., Kindermann, G., Kinoshita, T., Klein Goldewijk,
458 K., Riahi, K., Shevliakova, E., Smith, S., Stehfest, E., Thomson, A., Thornton, P., van Vuuren,
459 D. P., and Wang, Y.: Harmonization of Land-Use Scenarios for the Period 1500–2100: 600
460 Years of Global Gridded Annual Land-Use Transitions, Wood Harvest, and Resulting
461 Secondary Lands, *Climatic Change*, 109, 117–161, doi:10.1007/s10584-011-0153-2, 2011.

462 Jones, C. D., Hughes, J. K., Bellouin, N., Hardiman, S. C., Jones, G. S., Knight, J., Liddicoat,
463 S., O’Connor, F. M., Andres, R. J., Bell, C., Boo, K.-O., Bozzo, A., Butchart, N., Cadule, P.,
464 Corbin, K. D., Doutriaux-Boucher, M., Friedlingstein, P., Gornall, J., Gray, L., Halloran, P. R.,
465 Hurtt, G., Ingram, W. J., Lamarque, J.-F., Law, R. M., Meinshausen, M., Osprey, S., Palin, E.
466 J., Parsons Chini, L., Raddatz, T., Sanderson, M. G., Sellar, A. A., Schurer, A., Valdes, P.,
467 Wood, N., Woodward, S., Yoshioka, M., and Zerroukat, M.: The HadGEM2-ES
468 implementation of CMIP5 centennial simulations, *Geosci. Model Dev.*, 4, 543–570,
469 doi:10.5194/gmd-4-543-2011, 2011.

470 Kang, H.-S., D.-H. Cha and D.-K. Lee: Evaluation of the mesoscale model/land surface model
471 (MM5/LSM) coupled model for East Asian summer monsoon simulations, *J. Geophys. Res.*,
472 110, D10105, doi:10.1029/2004JD005266, 2005.

473 Kang, H.-S. and S.-Y. Hong: An assessment of the land surface parameters on the simulated
474 regional climate circulations: The 1997 and 1998 east Asian summer monsoon cases, *J.*
475 *Geophys. Res.*, 113, D15121, doi:10.1029/2007D009499, 2008.

476 Konaré, A., A. S. Zakey, F. Solmon, F. Giorgi, S. Rauscher, S. Ibrah, and X. Bi: A regional
477 climate modeling study of the effect of desert dust on the West African monsoon, *J. Geophys.*
478 *Res.*, 113, D12206, doi:10.1029/2007JD009322, 2008.

479 Lau, K. M., M.-T. Li: The monsoon of East Asia and its global associations-A survey, *B. Am.*
480 *Meteorol. Soc.*, 65, 114-125, 1984.

481 Lau, K. M., M. K. Kim, and K. M. Kim: Asian monsoon anomalies induced by aerosol direct
482 effects, *Clim. Dyn.*, 26, 855– 864, doi:10.1007/s00382-006-0114-z, 2006.

483 Lau, K. M and K.-M. Kim: Observational relationships between aerosol and Asian monsoon
484 rainfall, and circulation, *Geophys. Res. Lett.*, 33, L21810, doi:10.1029/2006GL027546, 2006.

485 Lawrence. D. M. and J. M. Slingo: An annual cycle of vegetation in a GCM. Part I:
486 implementation and impact on evaporation, *Clim. Dynam.*, 22, 87–105, doi:10.1007/s00382-
487 003-0366-9, 2004.

488 Lee, E., T. N. Chase, B. Rajagopalan, R. G. Barry, T. W. Biggs, and P. J. Lawrence: Effects of
489 irrigation and vegetation activity on early Indian summer and monsoon variability, *Int. J.*
490 *Climatol.*, 29, 573–581, doi:10.1002/joc.1721, 2009.

491 Lee, E., C. C. Barford, C. J. Kucharik, B. S. Felzer, and J. A. Foley: Role of turbulent heat
492 fluxes over land in the monsoon over East Asia, *Int. J. Geosci.*, 2, 420–431,
493 doi:10.4236/ijg.2011.24046, 2011.

494 Lee, E. J., S. W. Yeh, J. G. Jhun and B. K. Moon: Seasonal change in anomalous WNPSH
495 associated with the strong East Asian summer monsoon, *Geo. Res. Lett.*, 33, L21702, 2006.

496 Loveland, T. R., B. C. Reed, J. F. Brown, D. O. Ohlen, Z. Zhu, L. Yang, and J. W. Merchant:
497 Development of a global land cover characteristics database and IGBP DISCover from 1 km
498 AVHRR data, *Int. J. Remote Sensing*, 21, 1303–1330, doi:10.1080/014311600210191, 2000.

499 Martin, G. M. and R.C. Levine: The influence of dynamic vegetation on the present-day
500 simulation and future projections of the South Asian summer monsoon in the HadGEM2 family,
501 *Earth Syst. Dynam.*, 3, 245-261, doi:10.5194/esd-3-245-2012, 2012.

502 McCarthy, M. P., Sanjay, J., Booth, B. B. B., Krishna Kumar, K., and Betts, R. A.: The
503 influence of vegetation on the ITCZ and South Asian monsoon in HadCM3, *Earth Syst.*
504 *Dynam.*, 3, 87–96, doi:10.5194/esd-3-87-2012, 2012.

505 Miller, R. L., and I. Tegen: Climate response to soil dust aerosols, *J. Clim.*, 11, 3247–3267,
506 1998.

507 Paeth, H., and J. Feichter: Greenhouse-gas versus aerosol forcing and African climate response,
508 *Clim. Dyn.*, 26, 35– 54, 2005.

509 Qian Y, D. Gong, J. Fan, L. R. Leung, R. Bennartz, D. Chen and W. Wang: Heavy pollution
510 suppresses light rain in China: Observations and modeling, *J. Geophys. Res.*, 114, D00K02,
511 doi:10.1029/2008JD011575, 2009.

512 Ramanathan, V., C. Chung, D. Kim, T. Betge, L. Buja, J. T. Kiehl, W. M. Washington, Q. Fu,
513 D. R. Sikka, and M. Wild: Atmospheric brown clouds: Impacts on South Asian climate and
514 hydrological cycle, *Proc. Natl. Acad. Sci. U. S. A.*, 102, 5326 – 5333,
515 doi:10.1073/pnas.0500656102, 2005.

516 Seo K.-H, O. Ok J., J.-H. Son, D.-H. Cha: Assessing future changes in the East Asian summer
517 monsoon using CMIP5 coupled Models, *J. Clim.*, 26, 7662-7675, DOI: 10.1175/JCLI-D-12-
518 00694.1, 2013.

519 Sokolik I. N. and O. B. Toon: Direct radiative forcing by anthropogenic airborne mineral
520 aerosols, *Nature*, 381, 681-683, 1996.

521 Suh M.-S. and D.-K. Lee: Impacts of land use/cover changes on surface climate over east Asia
522 for extreme climate cases using RegCM2, *J. Geophys. Res.*, 109, D02108,
523 doi:10.1029/2003JD003681, 2004.

524 Taylor, K. E., Stouffer, R. J., and Meehl, G. A: An Overview of CMIP5 and the experiment
525 design, *B. Am. Meteorol. Soc.*, 93, 485–498, doi:10.1175/BAMS-D-11-00094.1, 2012.

526 The HadGEM2 Development Team: Martin, G. M., Bellouin, N., Collins, W. J., Culverwell, I.
527 D., Halloran, P. R., Hardiman, S. C., Hinton, T. J., Jones, C. D., McDonald, R. E., McLaren,
528 A. J., O'Connor, F. M., Roberts, M. J., Rodriguez, J. M., Woodward, S., Best, M. J., Brooks,
529 M. E., Brown, A. R., Butchart, N., Dearden, C., Derbyshire, S. H., Dharssi, I., Doutriaux-
530 Boucher, M., Edwards, J. M., Falloon, P. D., Gedney, N., Gray, L. J., Hewitt, H. T., Hobson,
531 M., Huddleston, M. R., Hughes, J., Ineson, S., Ingram, W. J., James, P. M., Johns, T. C.,
532 Johnson, C. E., Jones, A., Jones, C. P., Joshi, M. M., Keen, A. B., Liddicoat, S., Lock, A. P.,
533 Maidens, A. V., Manners, J. C., Milton, S. F., Rae, J. G. L., Ridley, J. K., Sellar, A., Senior, C.
534 A., Totterdell, I. J., Verhoef, A., Vidale, P. L., and Wiltshire, A: The HadGEM2 family of Met
535 Office Unified Model climate configurations, *Geosci. Model Dev.*, 4, 723-757,
536 doi:10.5194/gmd-4-723-2011, 2011.

537 Webster, P. J., Magana V. O., Palmer T. N., Shukla J., Tomas R. A., Yanai M. and Yasunari
538 T.: Monsoons: Processes, Predictability, and the Prospects for Prediction, *Journal of*
539 *Geophysical Research*, 3, 14451-14510. doi:10.1029/97JC02719, 1998.

540 Woodward, S.: Mineral dust in HadGEM2. Hadley Centre Technical Note 87, Met Office
541 Hadley Centre., Exeter, EX1 3PB, UK, available from
542 <http://www.metoffice.gov.uk/learning/library/publications/science/climate-science-technical->
543 [notes](http://www.metoffice.gov.uk/learning/library/publications/science/climate-science-technical-) (last access: 18 December 2014), 2011.

544 Xie, P., and P. A. Arkin: Global precipitation: A 17-year monthly analysis based on gauge
545 observations, satellite estimates, and numerical model outputs. *Bull. Amer. Meteor. Soc.*, 78,
546 2539 – 2558, 1997.

- 547 Yamashima, R., K. Takata, J. Matsumoto, and T. Yasunari: Numerical study of the impacts of
548 land use/cover changes between 1700 and 1850 on the seasonal hydroclimate in monsoon Asia,
549 J. Meteorol. Soc. Japan, 89A, 291–298, doi:10.2151/jmsj.2011-A19, 2011.
- 550 Yoshioka, M., N. M. Mahowald, A. J. Conley, W. D. Collins, D. W. Fillmore, C. S. Zender
551 and D. B. Coleman: Impact of desert dust radiative forcing on Sahel precipitation: relative
552 importance of dust compared to sea surface temperature variations, vegetation changes, and
553 greenhouse gas warming, J. Clim., 20, 1445-1467, DOI: 10.1175/JCLI4056.1, 2007.

554 Table 1. List of experiments.

555

Acronym	Description of the experiments	Time
A	HadGEM2-A	
AE	HadGEM2-A with ES vegetation	Present
Anod	HadGEM2-A with no dust radiative effects	1980-2005
AEnod	HadGEM2-A with ES vegetation with no dust radiative effects	
Ats	HadGEM2-A time slice run	
AEts	HadGEM2-A with ES vegetation time slice run	Future
AEnodts	HadGEM2-A with ES vegetation time slice run with no dust radiative effects	2080-2110

556

557 Table 2. Impacts of climate change of global warming, land cover change and dust loading
 558 obtained by the difference between the experiments in this study.

Impact	Descriptions
Climate change (Global warming)	$A_{ts} - A$
Climate change + LCC + Dust	$AE_{ts} - AE$
Climate change + LCC	$AE_{nodts} - AE_{nod}$
Dust	$(AE_{ts} - AE) - (AE_{nodts} - AE_{nod})$
LCC (ES land cover)	$(AE_{nodts} - AE_{nod}) - (A_{ts} - A)$

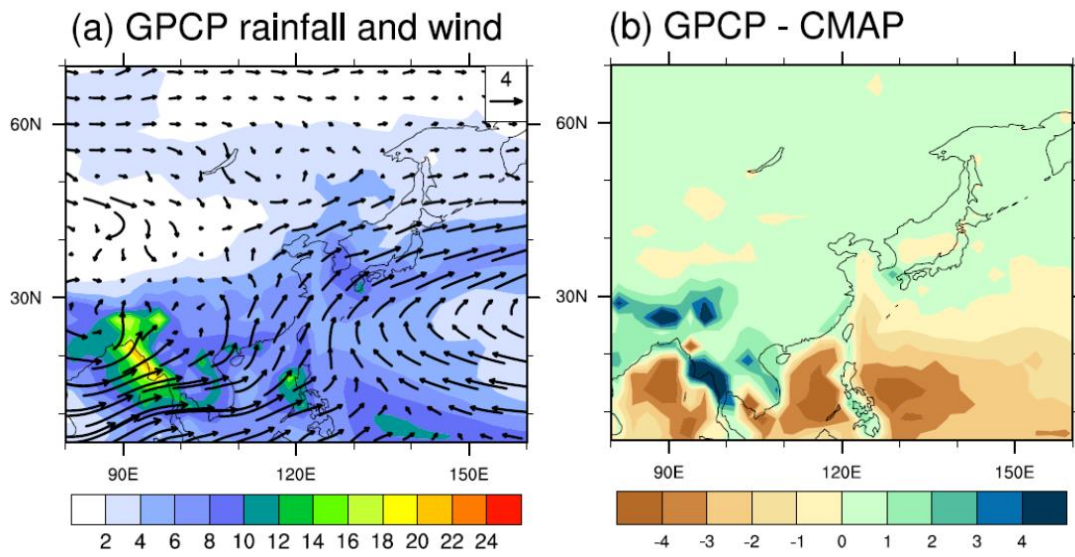
559

560

561

562

563



564

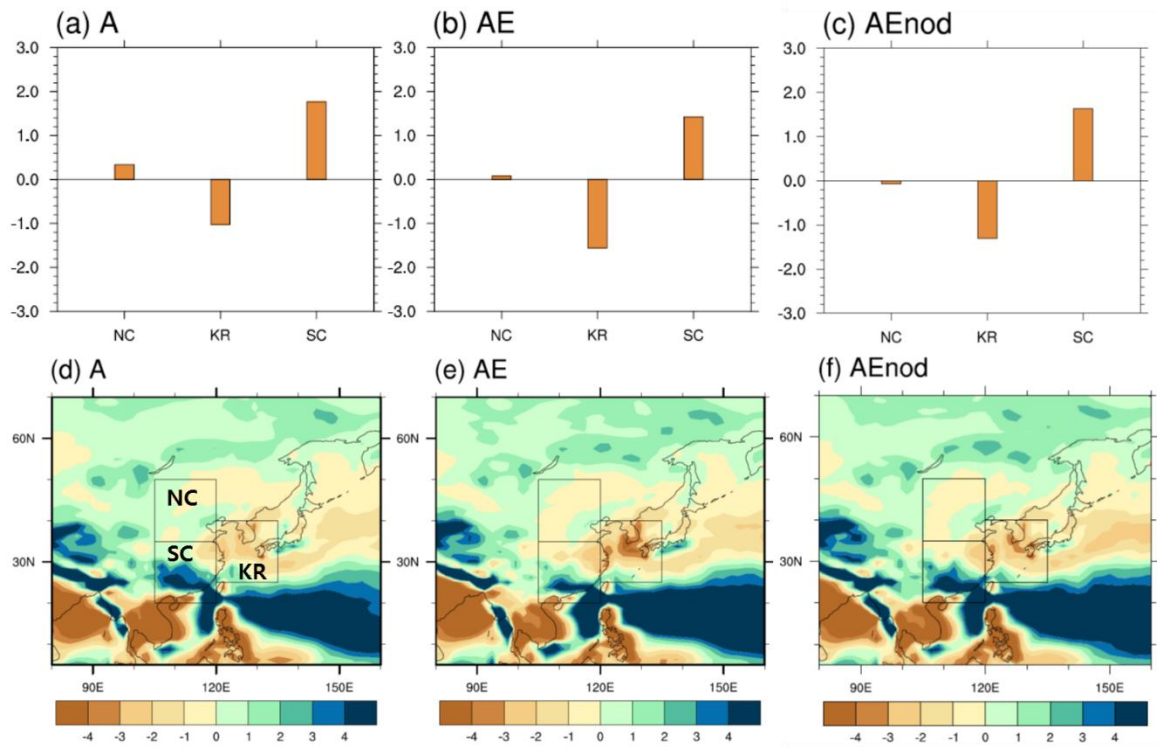
565

566 Figure 1. The 1982-2005 JJA (a) climatology of the Global Precipitation Climatology Project
 567 (GPCP) precipitation (mm day^{-1} , shading) and 850hPa winds (m s^{-1}) and (b) precipitation
 568 difference between GPCP and the CPC Merged Analysis of Precipitation (CMAP)

569

570

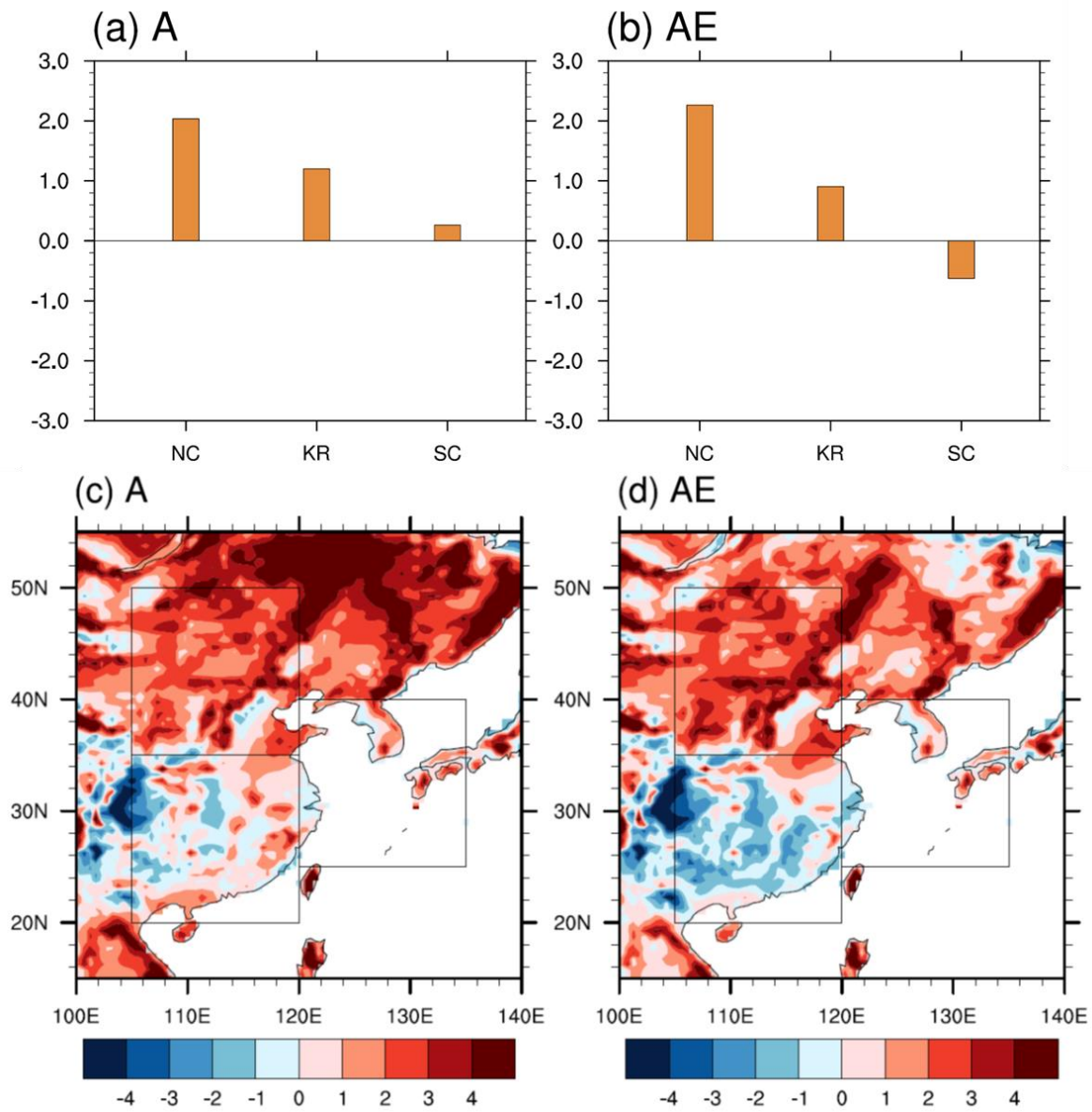
571



572

573 Figure 2. Area averaged JJA precipitation bias (mm day⁻¹) compared to the Global
574 Precipitation Climatology Project (GPCP) observation: (a, b and c) show regional mean
575 biases over the regions shown in (d, e and f). NC region: 35-50° N, 105-120° E; KR: 25-40°
576 N, 120-135° E; SC region: 20-35° N, 105-120° E.

577



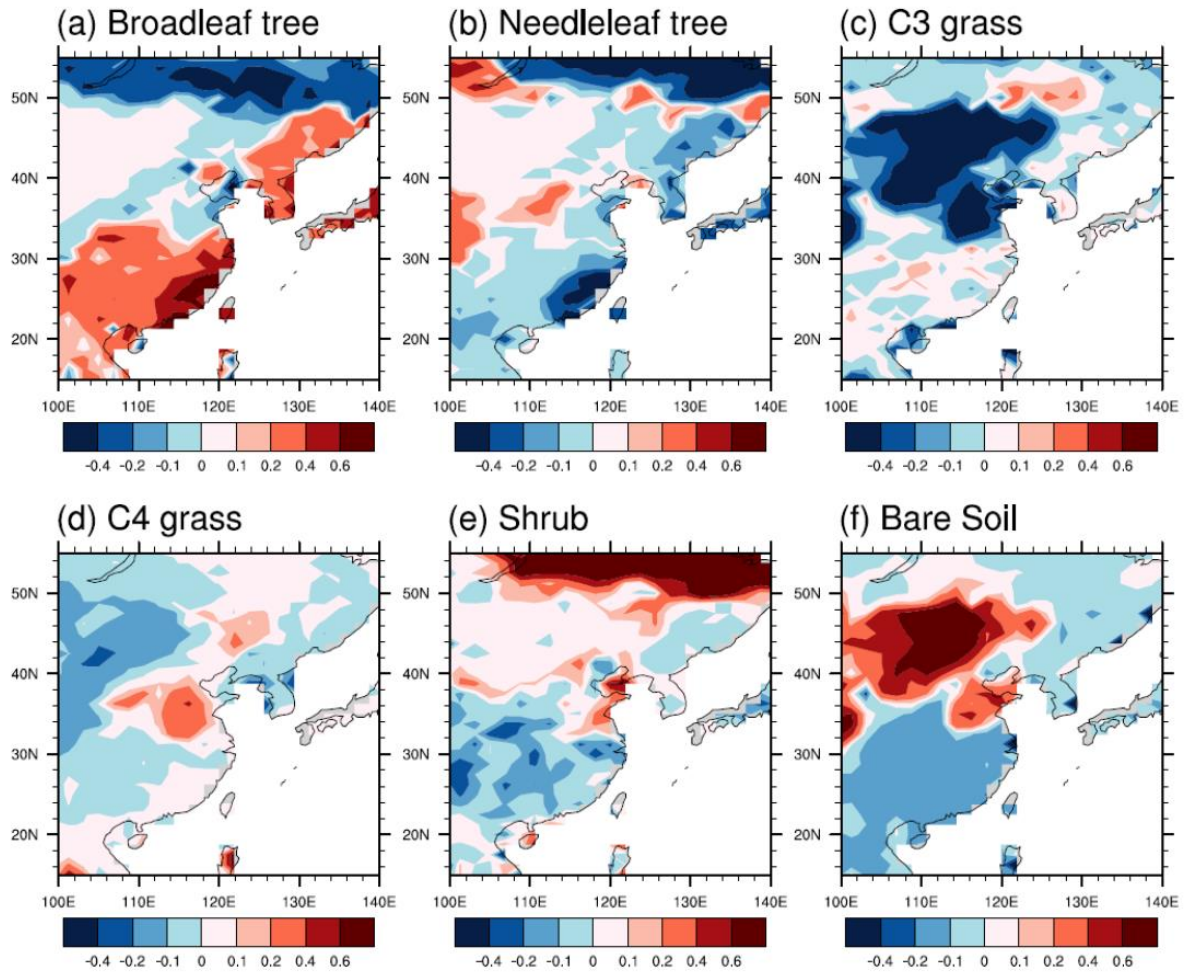
578

579

580 Figure 3. As Fig. 1 but for JJA surface air temperature biases (K) compared to the Climatic
 581 Research Unit (CRU) climatology.

582

583



584

585

586 Figure 4. Differences in present-day (1980-2005) fractions of land cover type between
 587 HadGEM2-ES and HadGEM2-AO (and HadGEM2-A) over East Asia.

588

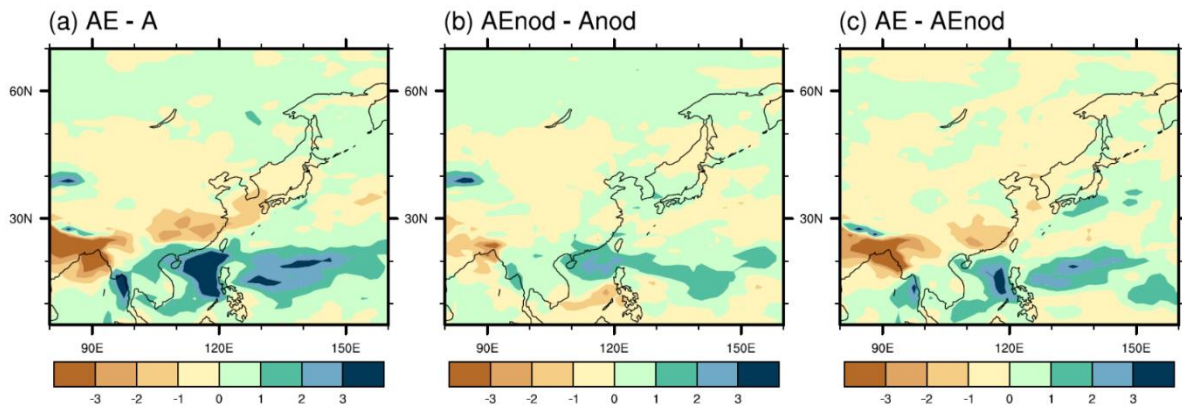
589

590

591

592

593



594

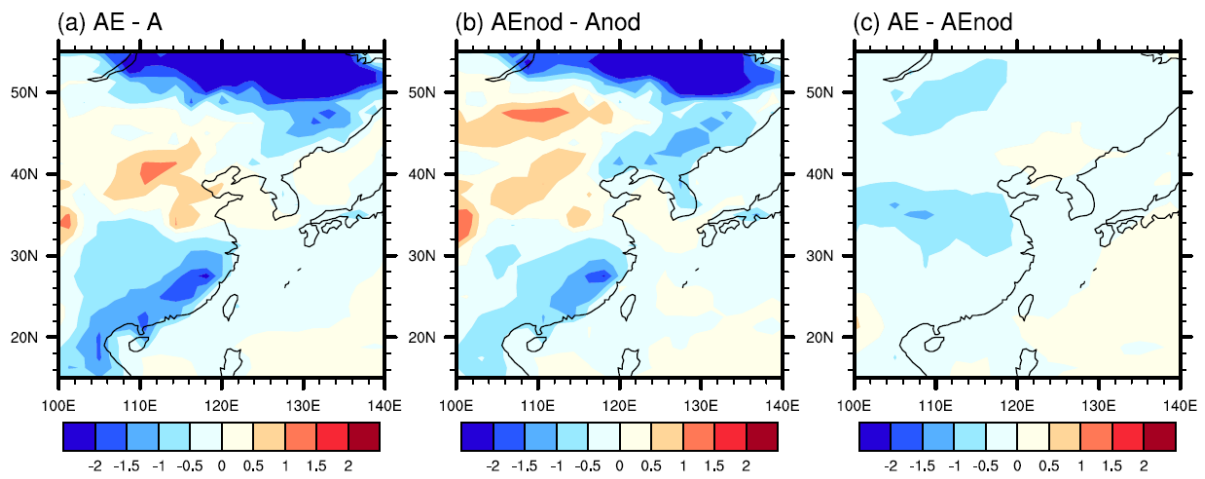
595

596 Figure 5. Precipitation differences (mm day^{-1}) in JJA for (a) AE minus A (b) AEnod minus
 597 Anod, and (c) AE minus AEnod.

598

599

600



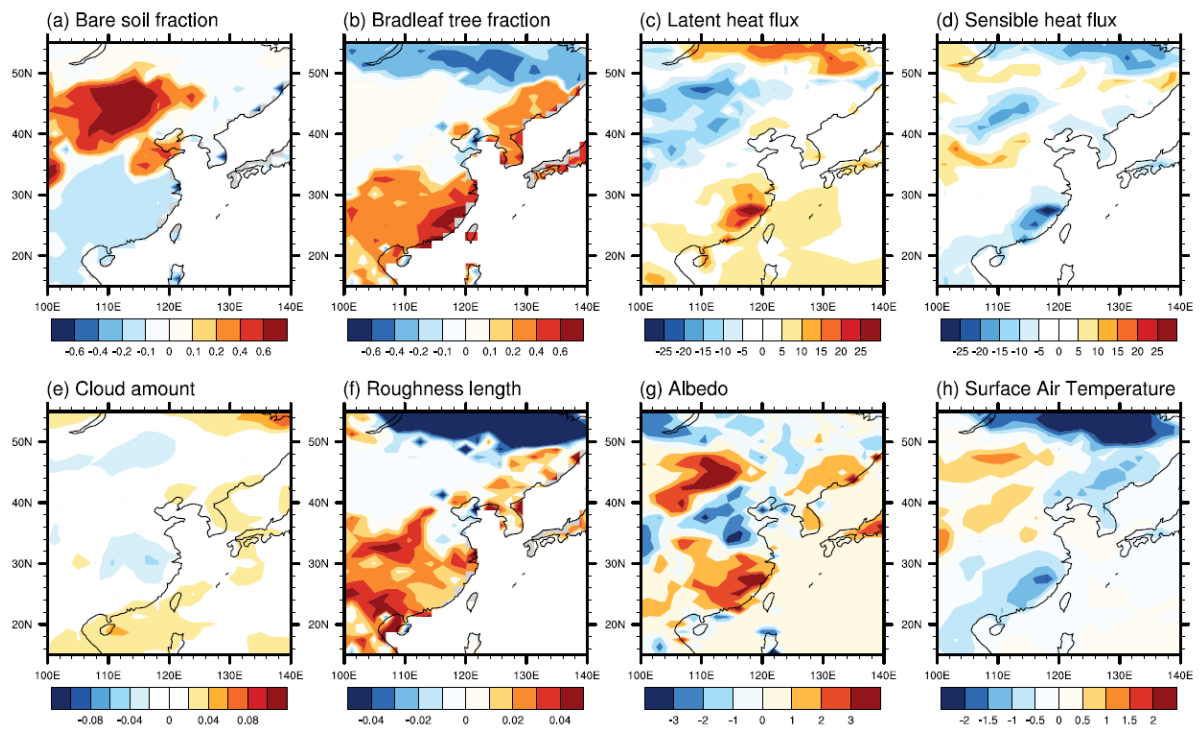
601

602

603 Figure 6. Surface air temperature differences (K) in JJA for (a) AE minus A, (b) AEnod
 604 minus Anod, (c) AE minus AEnod.

605

606

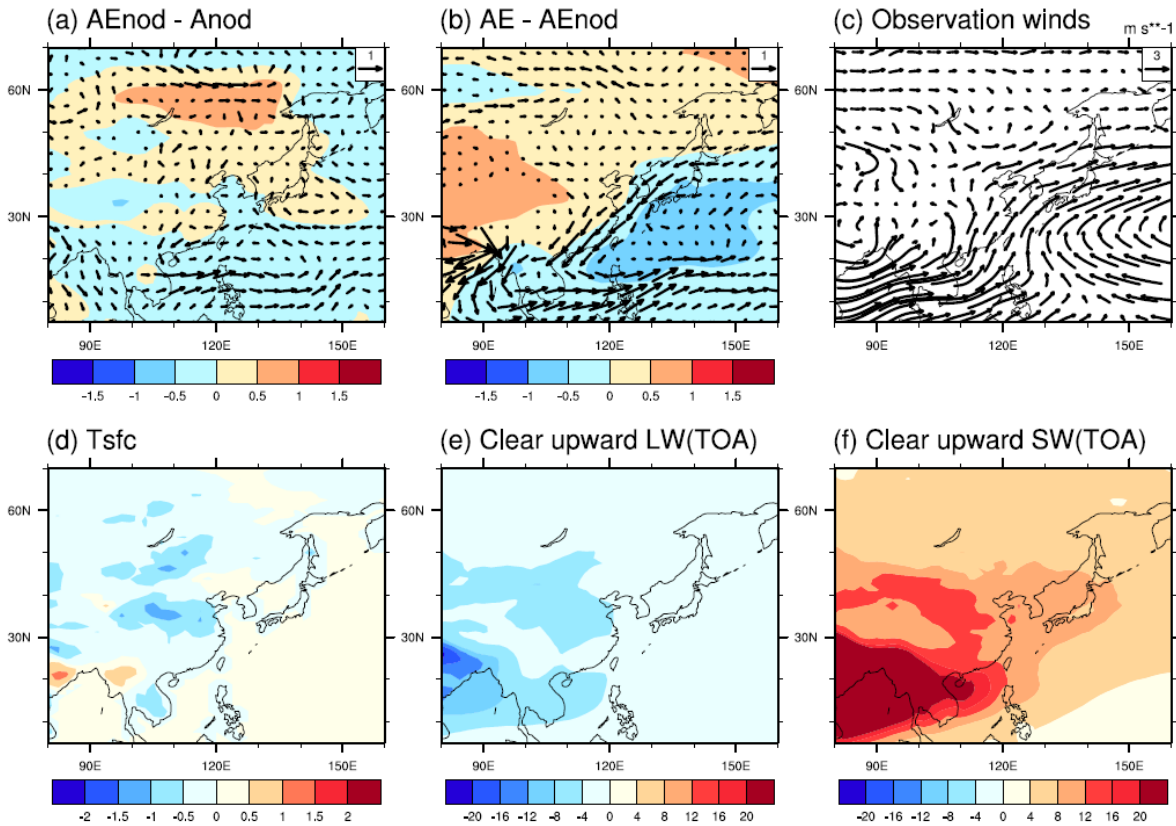


607

608 Figure 7. AEnod minus Anod in JJA showing the applied fractional land cover changes and
 609 their impact in (a) bare soil fraction, (b) broadleaf tree fraction, (c) latent heat flux (W m^{-2}), (d)
 610 sensible heat flux (W m^{-2}), (e) cloud amount (fraction), (f) roughness length (m), (g) albedo
 611 (%) and (h) surface air temperature (K).

612

613



614

615

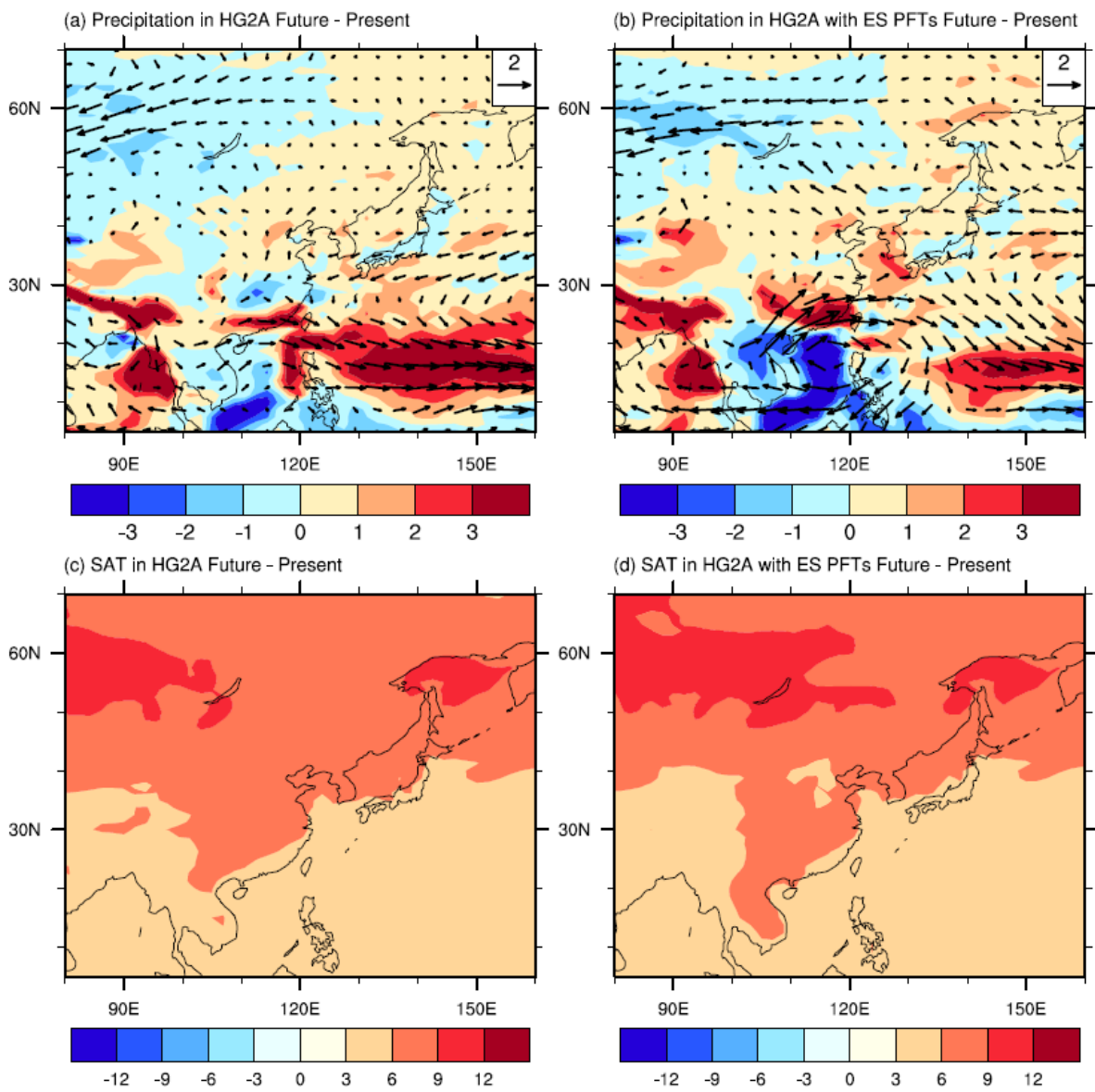
616 Figure 8. Changes in mean sea level pressure (hPa) and 850 hPa winds (m s^{-1}) in JJA for (a)
617 AEnod minus Anod, and (b) AE minus AEnod. (c) Climatology of 850 hPa winds for the period
618 1982-2005 using ERA Interim; (d to f) show differences between AE and AEnod in JJA: (d)
619 surface temperature (K), (e) clear sky upward longwave radiation (W m^{-2}) and (f) clear sky
620 upward shortwave radiation (W m^{-2}) at top of atmosphere, showing the impacts of the radiative
621 effects from additional dust loading induced by the ES land cover.

622

623

624

625

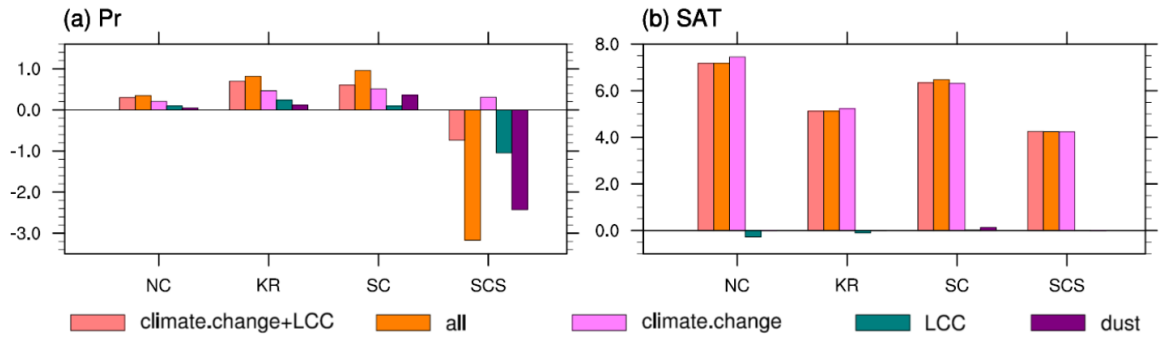


626

627

628 Figure 9. Changes in JJA mean precipitation (shading, mm day⁻¹) between future timeslice and
629 present-day HadGEM2-A experiments, without (a, c) and with (b, d) land cover from
630 HadGEM2-ES. (a), (c) is (Ats-A) and (b), (d) is (AEts-AE).

631

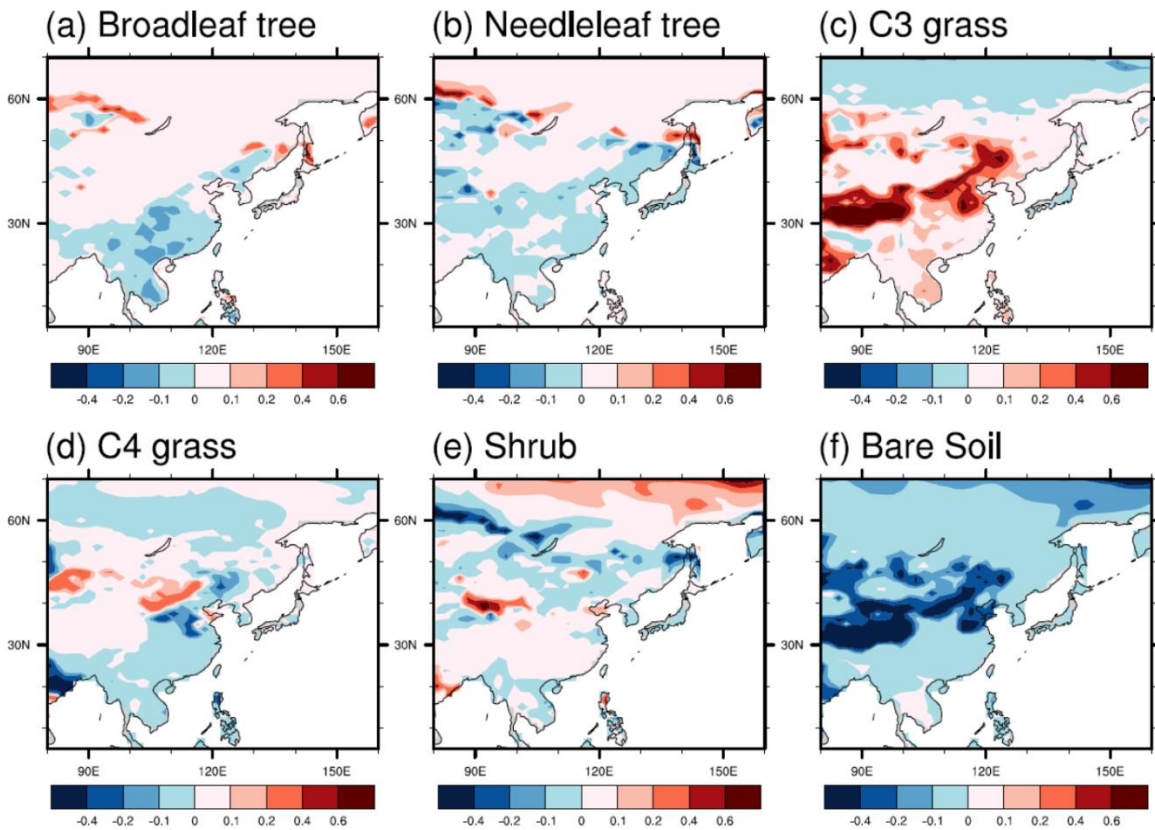


632

633 Figure 10. Future changes of precipitation (mm day⁻¹) (a) and surface air temperature (K) (b)
 634 over the box regions of North China (NC), Korea (KR), South China (SC) and South China
 635 Sea (SCS) in summer. Note that “all” means sum of climate change, land cover change and
 636 direct radiative effect of dust; “LCC” and “Dust” are ‘double-differences’ illustrating the
 637 influence of those processes on the future-present changes.

638

639

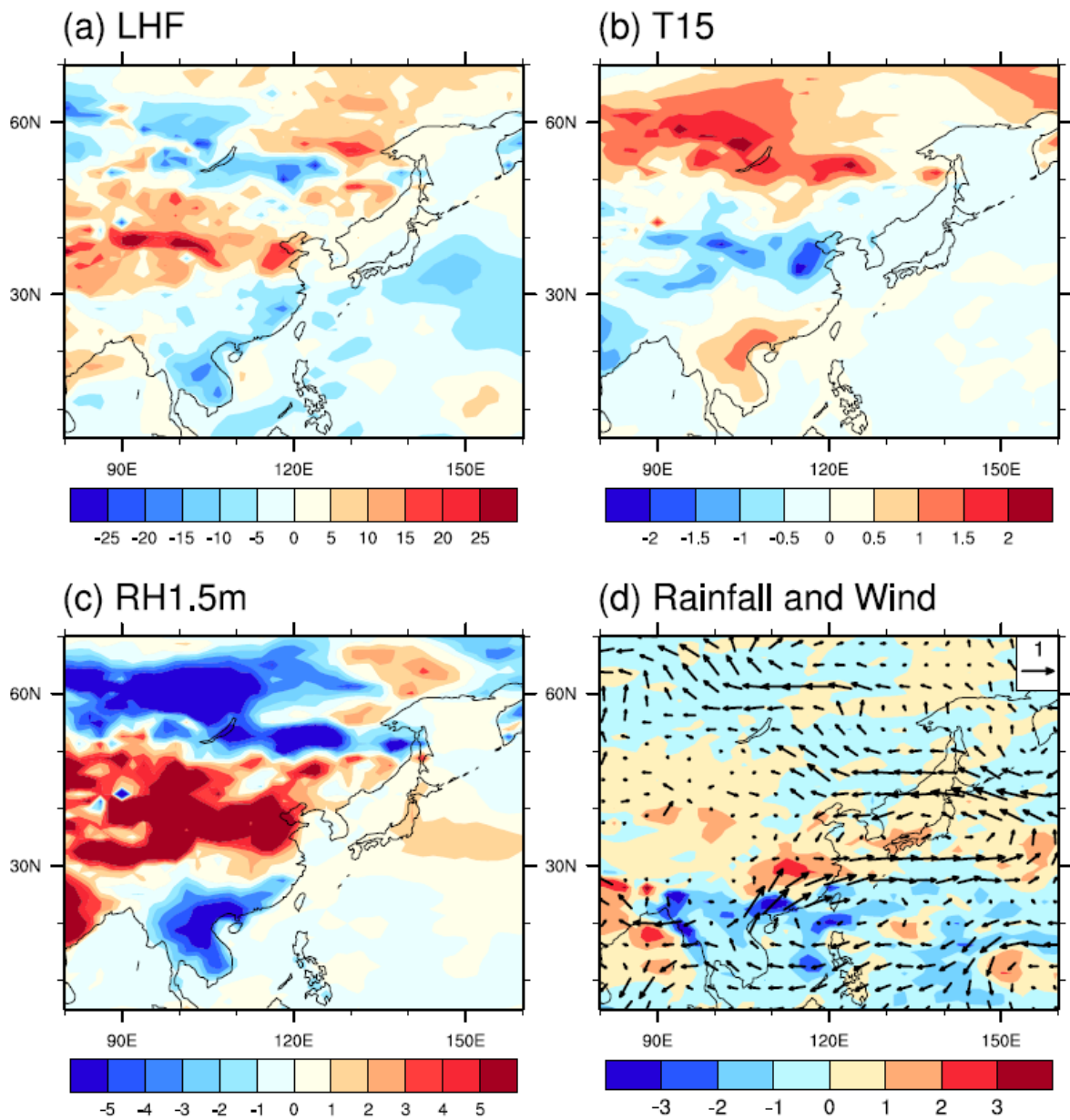


640

641

642 Figure 11. Changes of fractions in land cover between c.2100 and present-day as simulated by
 643 HadGEM2-ES in the Fifth Coupled Model Intercomparison Project (CMIP5) the
 644 Representative Concentration Pathway (RCP) 8.5 scenario and applied in AE present and AETs
 645 future time-slice experiments.

646

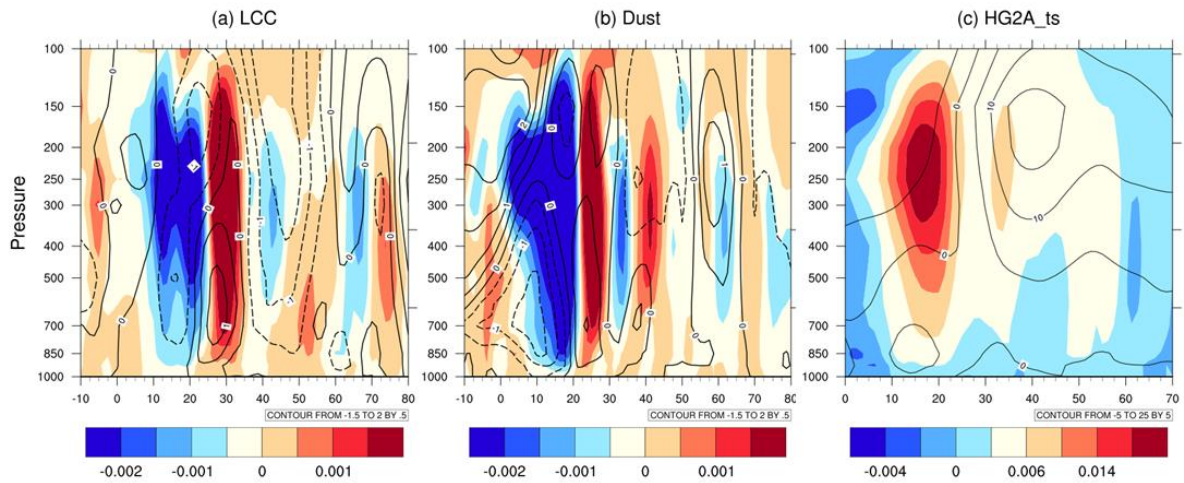


647

648

649 Figure 12. Contribution by the land cover changes alone to the future-present differences in
 650 JJA (represented by $(AEnodts - AEnod) - (Ats - A)$) in (a) latent heat flux ($W m^{-2}$), (b) surface
 651 air temperature (K), (c) 1.5 m relative humidity (%) and (d) rainfall (shading, $mm day^{-1}$), 850
 652 hPa wind (vectors, $m s^{-1}$).

653

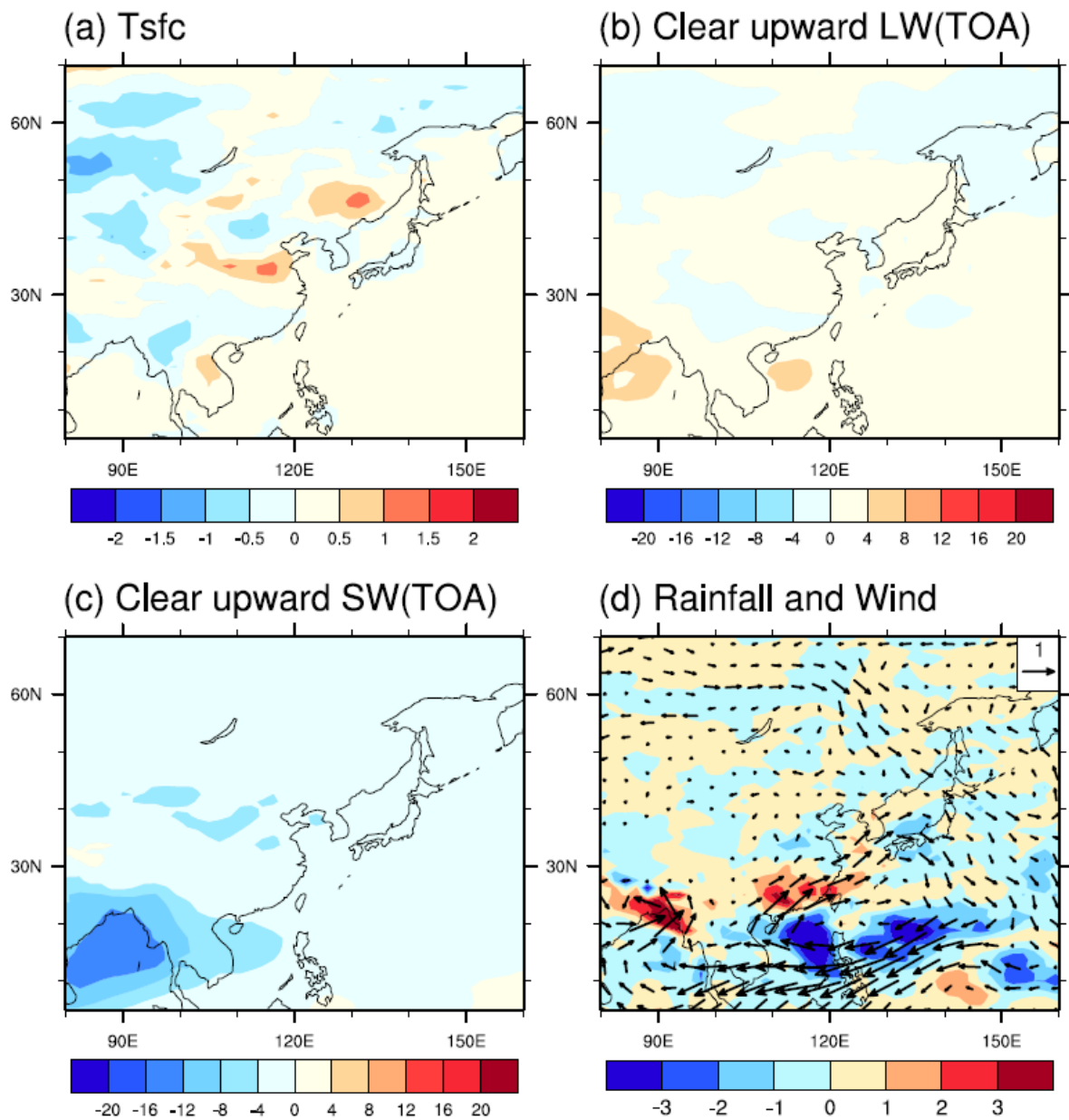


654

655

656 Figure 13. (a and b) Contribution to future-present changes in vertical motion (upward: red,
 657 downward: blue) and U wind anomalies (solid line: westerlies) from 110-120° E driven by
 658 (a) LCC impact, and (b) dust impact. (c) Climatological vertical motion over 110-120° E in
 659 the HadGEM2-A timeslice run, Ats.

660

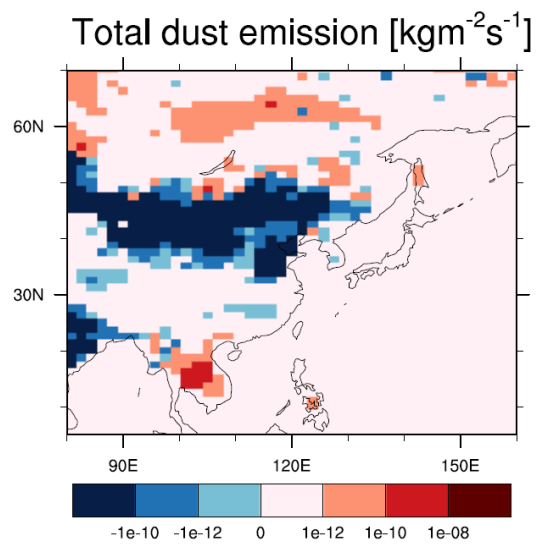


661

662

663 Figure 14. As Fig. 13 but showing the contribution from the direct radiative effect of dust to
 664 the future-present differences (represented by $(AE_{ts} - AE) - (AE_{nodts} - AE_{nod})$) in JJA in
 665 (a) surface temperature (K), (b) clear sky upward longwave radiation at top of atmosphere ($W m^{-2}$), (c)
 666 clear sky upward shortwave radiation at top of atmosphere ($W m^{-2}$) and (d) rainfall
 667 (shading, $mm day^{-1}$), 850 hPa wind (vectors, $m s^{-1}$).

668



669

670

671 Figure 15. Future changes in total dust emission ($\text{kg m}^{-2} \text{s}^{-1}$) in JJA from AETs – AE.

672